Progress In Electromagnetics Research C, Vol. 37, 171–182, 2013

COMPACT LOOP ANTENNA FOR NEAR-FIELD AND FAR-FIELD UHF RFID APPLICATIONS

Xiaozheng Lai[1, *], Zeming Xie[2], and Xuanliang Cen[2]

[1]School of Computer Science & Engineering, South China University of Technology, Guangzhou 510006, China

[2]School of Electronic & Information, South China University of Technology, Guangzhou 510641, China

Abstract—A novel type of radio frequency identification (RFID) reader antenna is proposed for mobile ultra-high frequency (UHF) RFID device. By folded-dipole loop structure with parasitic element, a small antenna size of $31 * 31 * 1.6\,\text{mm}^3$ is achieved. The antenna with different parasitic element size can work on different UHF RFID bands. The antenna prototype is fabricated and the measured bandwidth is around 13.5 MHz (915.5–929 MHz), which covers the China RFID Band (920–925 MHz). The measured reading distance achieves 65 mm with the near-field RFID tag and 1.17 m with the far-field tag. The measurement agrees well with simulated result and shows that antenna is desirable for both near-field and far-field UHF RFID applications.

1. INTRODUCTION

Radio-frequency-identification (RFID) technology has received a lot of attention in warehouse, supply chain, industry, and commerce [1]. As RFID deployment moves from pallet level to item level, it is necessary to identify and track objects by RFID tags at anytime and anywhere. Then, mobile RFID device has advantages in terms of cost, portability and wireless communication. Mobile RFID device is defined as a compact RFID reader into a mobile phone, which provides diverse services through mobile communication networks [2]. Anyone with mobile RFID device can directly identify RFID tags attached object, and access cloud computing with 3G/WiFi communication network for searching, verifying, and managing object information. Mobile RFID has been a rapidly growing RFID technology for item-level tagging

Received 31 December 2012, Accepted 6 February 2013, Scheduled 7 February 2013

* Corresponding author: Xiaozheng Lai (laixz@scut.edu.cn).

(ILT) in different applications, such as pharmaceutical and retailing industry [3].

However, the challenge of mobile RFID is that the mobile reader antenna must have both near-field and far-field RFID operation for various applications. Inductively coupled near-field operation is usually used for objects surrounded by metals or liquids [4]. Then electromagnetically far-field operation is commonly used to achieve long reading range [5]. The near-field RFID system is conventionally used at low frequency (LF, 125–134 kHz), high frequency (HF, 13.56 MHz), and ultra-high frequency (UHF, 840–960 MHz) bands, but far-field RFID systems only operate at UHF band [6]. Thus, RFID system for both near-field and far-field applications at UHF band simultaneously is drawing the world's attention.

The typical UHF RFID reader antenna works with pure far-field characteristic [7–10]. Recently, a few UHF reader antennas have been considered with pure near-field characteristic [11–16]. But there are few papers about antenna for both near-field and far-field UHF operations, and they all have too large size to use in mobile: one has a dimension of $184 * 174\,\mathrm{mm}^2$ [17], another smaller antenna is $72.3 * 72.3\,\mathrm{mm}^2$ [18].

In this paper, we present a novel type of folded-dipole loop antenna, with two parasitic C-type elements. The antenna can operate on Europe Band, China Band and Japan Band, by modifying the parasitic element parameters. The antenna prototype is fabricated and achieves a special small size of $31 * 31\,\mathrm{mm}^2$. The measured 10 dB bandwidth is 13.5 MHz (915.5–929 MHz), which covers the China RFID band (920–925 MHz). The reading capability of antenna is up to 65 mm with near-field RFID tag and up to 1.17 m with far-field RFID tag. Simulation and measurement show that the proposed antenna has available far-field gain,strong current and uniform magnetic near-field distribution.

The organization of this paper is as follows: The proposed antenna structure is introduced in Section 2. Section 3 outlines the simulation and measurement of antenna. Section 4 presented the near-field and far-field read range measurements. The conclusion is given in Section 5.

2. ANTENNA DESIGN AND STRUCTURE

Loop antennas are commonly used for mobile systems [19–23]. At LF and HF bands, a physically large loop is still a very small electrically fraction compared to the operating wave-length. So the conventional RFID antenna design at LF and HF bands is to use multiturn loop. However, it is not suggested at UHF band, because the multiturn loop

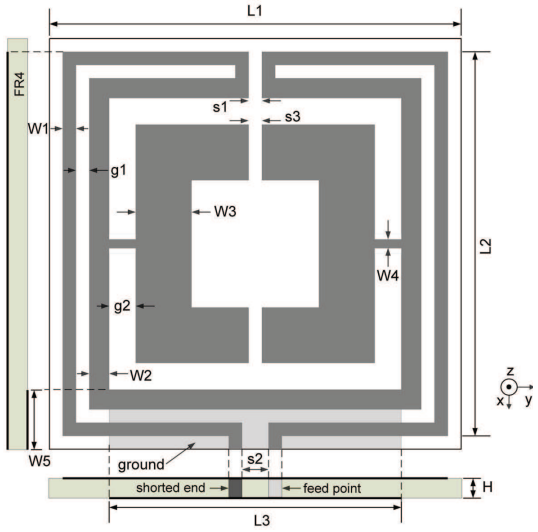

Figure 1. Geometry of the proposed antenna.

or spiral inductor has poor far-field gain. The other way is to use folded-dipole loop [24]. The folded-dipole loop antenna has good size reduction and exhibits better far-field gain than multiturn loop.

In this paper, a novel folded-dipole antenna with parasitic element is proposed, as shown in Fig. 1. The bent folded-dipole forms a large outer loop with a split, and two C-type arms combine a small inner loop with two splits. The antenna geometry was designed on a 1.6 mm-thick low-cost substrate with $\varepsilon_r = 4.4$ and the whole antenna size is L_1 (31 mm) $\times$ L_1 (31 mm). The dimension of the proposed antenna is as shown in Table 1.

One of the advantages of folded-dipole loop is that the input impedance can be adjusted by the parasitic element [25]. Fig. 2 shows the simulated input impedance against frequency by varying the C-type arm parameters. The 50 Ω line of resistance is shown in Fig. 2(a) and 0 Ω line of reactance in Fig. 2(b). It is first noted that the impedance curve is almost unchanged, but shifted to higher or lower frequency by adjusting the parasitic element parameter. When $s_3 = 1.0$ mm, and $W_4 = 0.9$ mm, the input impedance of $46.2 - j9.9\,\Omega$ is obtained at 920 MHz, which almost achieves the matching goal of $50 + j0\,\Omega$. By decreasing the width W_4 or split s_3, the input resistance and reactance curve are both shifted to lower frequency. By increasing the width W_4 or split s_3, the input resistance and reactance curve are both shifted to higher frequency.

Table 1. Dimensions of proposed antenna (unit: mm).

Antenna square edge	L_1	31.0
Folded-dipole loop	L_2	29.0
	W_1	1.0
	W_2	1.5
	g_1	1.0
	s_1	1.0
	s_2	2.0
C-type arm	W_3	4.2
	W_4	0.9
	g_2	2.0
	s_3	1.0
Metal ground	L_3	22.0
	W_5	4.5

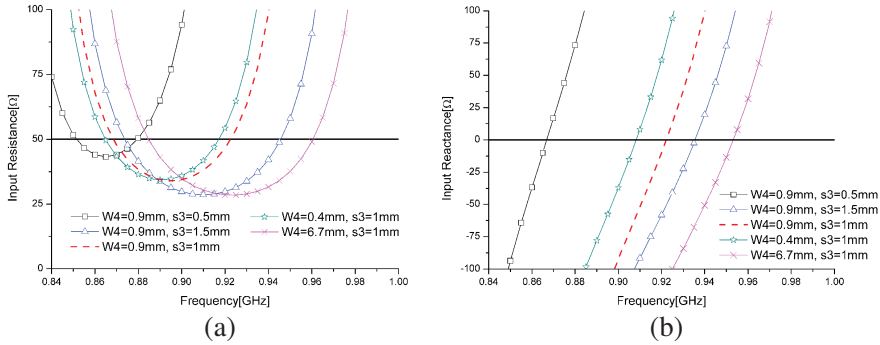

Figure 2. Input impedance with various parasitic element. (a) Resistance. (b) Reactance.

Figure 3 presents the parametric sweep of the proposed and conventional antenna. The parasitic element significantly lowers resonance frequency of the folded-dipole loop. Compared to the conventional antenna, the proposed antenna in Fig. 1 and Table 1 has an enough bandwidth for China RFID Band (920–925 MHz), with $s_3 = 1.0$ mm, and $W_4 = 0.9$ mm. This antenna is also suitable for Korea RFID Band (917–924 MHz) and Australia RFID Band (918–926 MHz). When the split s_3 lowers to 0.5 mm, the antenna will operate well on Europe RFID Band (865–868 MHz). However, if the width W_4

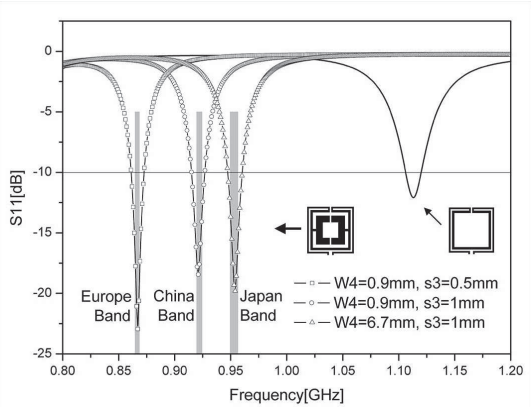

Figure 3. Parametric sweep of the proposed and conventional antenna.

is enhanced with a larger value of 6.7 mm, the bandwidth of antenna will completely cover Japan RFID Band (950–956 MHz). Therefore, the proposed antenna can be customized for different RFID bands by varying the parasitic element parameters.

3. SIMULATION AND EXPERIMENTAL RESULTS

A prototype of the proposed antenna was fabricated, as shown in Fig. 4. The entire area of prototype is just $31 \times 31\,\text{mm}^2$, as a coin of one CNY. Simulations of the proposed antenna were performed using Ansoft High Frequency Structure Simulator (HFSS) software, which uses the finite element method (FEM).

The comparison of simulated and measured S-parameter is shown in Fig. 5(a). The measured bandwidth of the antenna prototype is 13.5 MHz (915.5–929 MHz), under the condition of reflection coefficient less than -10 dB, which covers the China RFID Band (920C–925 MHz) completely. In Fig. 5(a), the antenna prototype exhibits a measured -30.5 dB result, which is better than the simulated result. The discrepancy is mainly due to the feeder line and SMA connector as shown in Fig. 4, which size is similar to the antenna prototype. Since the antenna ground is often connected to PCB in application, we consider the effect of SMA connector equivalent to the PCB ground. Fig. 5(b) shows the measured gain at the X-axis versus frequency, which were obtained by the anechoic chamber. The fabricated antenna had a gain of $-4.4 \sim -5.0$ dBi over the China RFID Band (920–925 MHz).

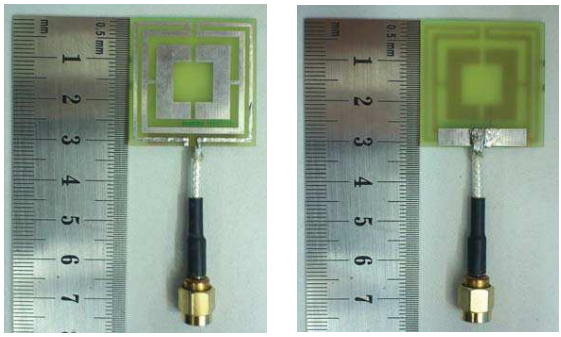

(a) (b)

Figure 4. Fabricated proposed antenna prototype. (a) Top view. (b) Bottom view.

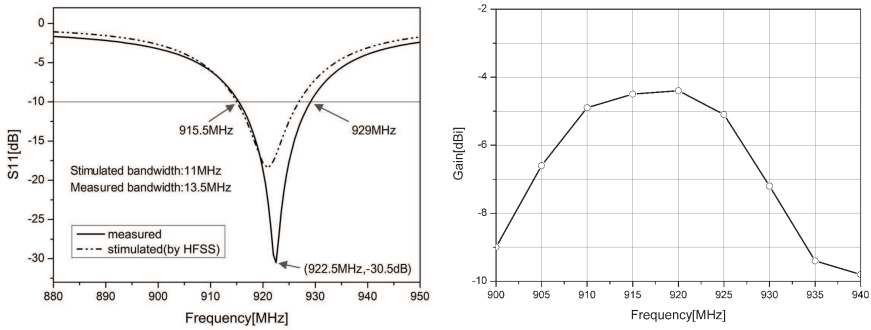

(a) (b)

Figure 5. (a) Simulated and measured S-parameter. (b) Measured gain at the X-axis.

The simulation result of antenna surface current distribution at 922 MHz is shown in Fig. 6(a), and the magnetic field above antenna at xy-plane and $z = 20$ mm is demonstrated, as shown in Fig. 6(b). It can be seen that in-phase current is flowing along the folded dipole-loop and most edge of parasitic loop, except the current at the lower edge of parasitic loop. Though the current at the lower edge of folded dipole-loop is at least double larger in amplitude relative to that of parasitic loop as shown in Fig. 6(a), the whole current distribution still enables a uniform and sufficient strong magnetic field distribution on the near-field antenna region as shown in Fig. 6(b).

The simulated and measured radiation patterns of the proposed antenna are plotted in Fig. 7. The measured radiation patterns were

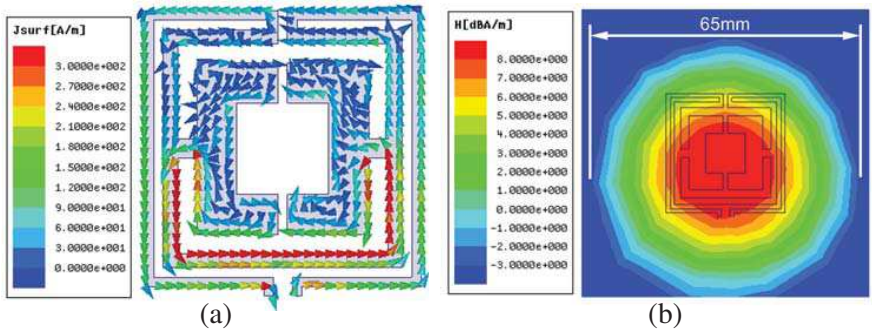

Figure 6. (a) Antenna surface current distribution. (b) Near-field magnetic distribution (xy-plane, $z = 20\,\text{mm}$).

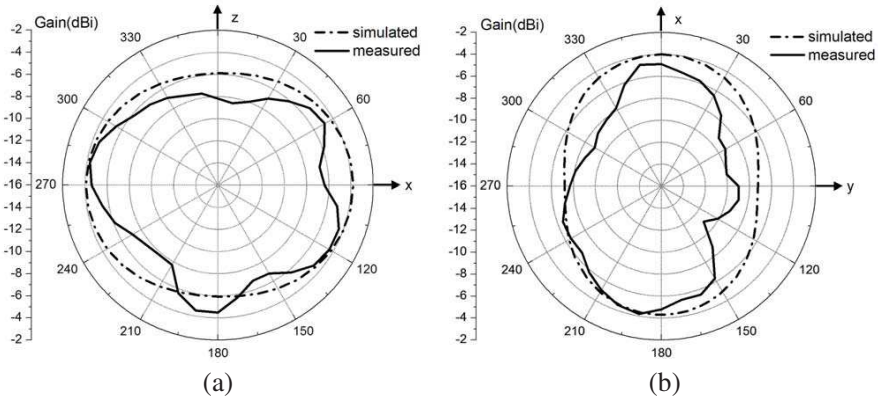

Figure 7. Simulated and measured far-field radiation patterns. (a) H-plane (xz-plane), (b) E-plane (xy-plane).

obtained by the anechoic chamber. Figs. 7(a) and (b) show the radiation patterns at 922 MHz in the two orthogonal planes (E-plane and H-plane). The far-field gain of proposed antenna achieves the maximum gain of $-4.4\,\text{dBi}$ at the bidirectional X-axis and negative Z-axis, which shows that the proposed antenna can be acceptable for far-field RFID application.

4. NEAR-FIELD AND FAR-FIELD READING MEASUREMENTS

The measurement of near-field reading range is presented in Fig. 8. The Impinj UHF button of $13 * 10\,\text{mm}^2$ dimension was taken as the

reference tag, and the Impinj Technology Speedway R420 reader was used to feed the proposed antenna structure. The test scene is shown in Fig. 8(b). The proposed antenna prototype is fabricated on the test stand, and the near-field button tag, attached to polyfoam, is parallel to the surface of antenna. The schematic view is shown in Fig. 8(a). The reading range d between antenna and tag is achieved along the positive Z-axis.

The read capability of near-field antenna includes read-range and read-width. With Impinj UHF button parallel to the prototype, the maximum read range can reach 65 mm along the positive Z-axis under the transmission power level of 20 dBm. Figs. 9(a) and (b) show that the measured read widths of xy-plane are 65 mm at $z = 20$ mm, and 5 mm at $z = 65$ mm (maximum distance). The read width at $z = 20$ mm agrees well with the simulated results of magnetic field

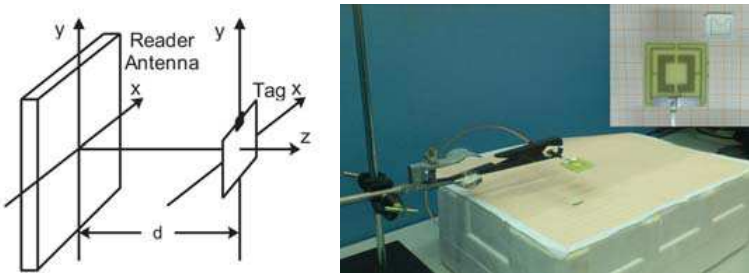

(a) (b)

Figure 8. Near-field measurement. (a) Schematic view. (b) Test scene.

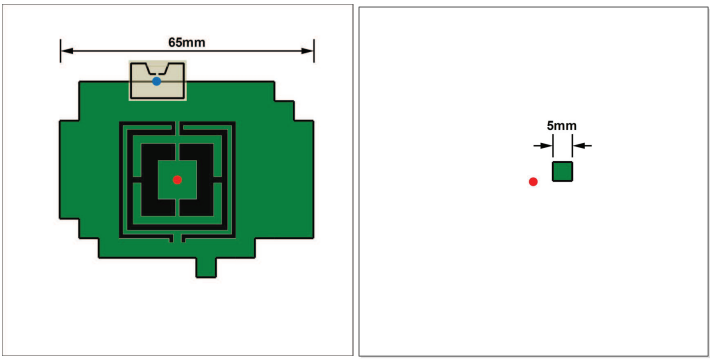

(a) (b)

Figure 9. Measured results of read width at xy-plane. (a) $z = 20$ mm. (b) $z = 65$ mm (maximum distance).

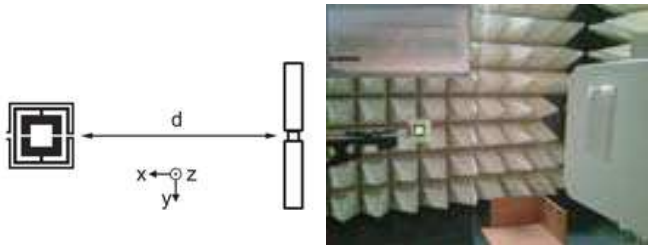

(a) (b)

Figure 10. Far-field measurement. (a) Schematic view. (b) Test scene.

Table 2. Near- and far-field maximum reading range in different environment (unit: mm).

Environment	Transmission Power@20 dBm		Transmission Power@10 dBm	
	Near-field Scene	Far-field Scene	Near-field Scene	Far-field Scene
Air	65	1170	45	178
Water Container	70	310	36	95
Paper (book)	60	350	32	65
Fruit Surface (apple)	65	120	55	30
Skin Surface (human)	45	45	20	12

distribution in Fig. 6(b).

The test scene of far-field reading range in the anechoic chamber is presented in Fig. 10(b). A common dipole tag is taken as the reference tag, and the Impinj Technology Speedway Reader feeds the proposed antenna. The reading range d, as shown in Fig. 10(a), achieves 1.17 m along the negative X-axis by transmission power of 20 dBm.

Furthermore, the maximum reading range of proposed antenna is measured under the different environment. The near-field maximum range was measured along the positive Z-axis of antenna, and test scene is shown in Fig. 8. The far-field maximum range was measured along the negative X-axis of antenna, and test scene is shown in Fig. 10. In Table 2, we can see the measured results with the near-field and far-field tag attached on the surface of different objects, including air, liquids, paper, plant and human body. The maximum far-field range achieves 1.17 m under the transmission power level of 20 dBm (0.1 W).

But the different object seriously affects the read performance of far-field tag. When the far-field tag is attached to water-item container (liquid) or conducting plate (human body), the reading range reduces rapidly. On the contrary, the maximum reading range with the near-field tag attached to the other objects is similar to that in the air. It is a major advantage of the near-field RFID system.

5. CONCLUSIONS

In this paper, a novel compact loop antenna is proposed. Owing to parasitic C-type arms inserted to folded-dipole loop, the proposed antenna realized good size reduction, uniform magnetic near-field distribution and available far-field gain. Further, the parasitic element of proposed antenna can be modified to handle different UHF RFID bands in this article.

Finally, the antenna prototype, with a compact size of $31 * 31 * 1.6\,\text{mm}^3$, provides 13.5 MHz bandwidth (915.5C–929 MHz), which can cover the China RFID band (920–925 MHz) completely. With a near-field button-type RFID tag, the maximum read range obtained is 65 mm. The near-field reading performance is not degraded when the RFID tag is placed on different objects (liquid, paper, fruit surface and human body). On the other hand, the far-field reading range, with a common dipole RFID tag, is approximately 1.17 m, but the performance is seriously affected by surrounding. Such an antenna design has suitable near-field and far-field performance for mobile UHF RFID application.

ACKNOWLEDGMENT

This paper is supported by the National High Technology Research and Development Program (863 program) of China (2008AA04A103), Science and Technology Planning Project of Guangdong Province (2011B080701068), and National Natural Science Foundation of China (61101015 & 60971052).

REFERENCES

1. Finkenzeller, K., *RFID Handbook: Radio-frequency Identification Fundamentals and Applications*, 2nd Edition, Wiley, New York, 2004.
2. Chae, J. and S. Oh, "Information report on mobile RFID in Korea," ISO/IEC JTC1/SC 31/WG4 N0922, Information Paper, ISO/IEC JTC1 SC31 WG4 SG5, 2005.

3. Lee, J. and H. Kim, "RFID code structure and tag data structure for mobile RFID services in Korea," *Proc. ICACT*, 1053–1055, Feb. 2006.
4. Fuschini, F., C. Piersanti, L. Sydanheimo, L. Ukkonen, and G. Falciasecca, "RFID code structure and tag data structure for mobile RFID services in Korea," *IEEE Trans. Antennas Propag.*, Vol. 58, No. 5, 1759–1770, Dec. 2010.
5. Razalli, M. S., M. A. Mahdi, A. Ismail, S. M. Shafie, and H. Adam, "Design and development of wireless communication transceiver to support RFID reader at UHF band," *Journal of Electromagnetic Waves and Applications*, Vol. 24, Nos. 14–15, 2063–2075, 2010.
6. Nikitin, P. V., K. V. S. Rao, and S. Lazar, "An overview of near field UHF RFID," *Proc. IEEE Int. Conf. on RFID*, 167–174, Mar. 2007.
7. Lee, J. N. and J. H. Jung, "Design of the planar cross dipole reader antenna for UHF RFID systems," *Journal of Electromagnetic Waves and Applications*, Vol. 26, No. 7, 962–972, 2012.
8. Viani, F., M. Salucci, F. Robbl, G. Oliveri, and A. Massa, "Design of a UHF RFID/GPS fractal antenna for logistics management," *Journal of Electromagnetic Waves and Applications*, Vol. 26, No. 4, 480–492, 2012.
9. Wang, P., G. Wen, J. Li, Y. Huang, and Q. Zhang, "Wideband circularly polarized UHF RFID reader antenna with high gain and wide axial ratio beamwidth," *Progress In Electromagnetics Research*, Vol. 129, 365–385, 2012.
10. Tiang, J. J., M. T. Islam, N. Misran, and J. S. Mandeep, "Circular microstrip slot antenna for dual-frequency RFID application," *Progress In Electromagnetics Research*, Vol. 120, 499–512, 2011.
11. Wang, L., Z. J. Xing, J. Y. Li, K. Wei, M. S. Sandikie, and J. D. Xu, "Fast carrier cancellation for UHF near field RFID system," *Journal of Electromagnetic Waves and Applications*, Vol. 26, No. 7, 863–874, 2012.
12. Li, X. and Z. Yang, "Dual-printed- dipoles reader antenna for UHF near-field RFID applications," *IEEE Antennas Wireless Propag. Lett.*, Vol. 10, 239–242, 2011.
13. Lai, X. Z., Z. M. Xie, Q. Q. Xie, and J. M. Chao, "A SRR-based near field RFID antenna," *Progress In Electromagnetics Research C*, Vol. 33, 133–144, 2012.
14. Qing, X., C. K. Goh, and Z. N. Chen, "A broadband UHF near-field RFID antenna," *IEEE Trans. Antennas Propag.*, Vol. 58, No. 12, 3829–3838, Dec. 2010.

15. Xie, Z. M., X. Z. Lai, and R. J. Hu, "Compact UHF RFID reader antenna using bended fold dipole structure," *International Conference on Machine Learning and Cybernetics*, Vol. 1, 414–417, Jul. 2011.
16. Li, X., J. Liao, Y. Yuan, and D. Yu, "Eye-shaped segmented reader antenna for near-field UHF RFID applications," *Progress In Electromagnetics Research*, Vol. 114, 481–493, 2011.
17. Shrestha, B., A. Elsherbeni, and L. Ukkonen, "UHF RFID reader antenna for near-field and far-field operations," *IEEE Antennas Wireless Propag. Lett.*, Vol. 10, 1274–1277, Nov. 2011.
18. Borja, A. L., A. Belenguer, J. Cascon, and J. R. Kelly, "A reconfigurable passive UHF reader loop antenna for near-field and far-field RFID applications," *IEEE Antennas Wireless Propag. Lett.*, Vol. 11, 580–583, Nov. 2012.
19. Lin, D. B., C. C. Wang, J. H. Chou, and I. T. Tang, "Novel UHF RFID loop antenna with interdigital coupled section on metallic objects," *Journal of Electromagnetic Waves and Applications*, Vol. 26, Nos. 2–3, 366–378, 2012.
20. Xiong, J., Y. F. Yu, Y. M. Liu, and X. Geng, "An electrically small planar loop antenna with high efficiency for mobile terminal applications," *Journal of Electromagnetic Waves and Applications*, Vol. 26, Nos. 5–6, 744–756, 2012.
21. Yu, H. Z. and Q. X. Chu, "An omnidirectional small loop antenna based on first-negative-order resonance," *Journal of Electromagnetic Waves and Applications*, Vol. 26, No. 1, 111–119, 2012.
22. Lin, Y. C., W. S. Chen, B. Y. Lee, S. Y. Lin, and H. W. Wu, "Small inverted-U loop antenna for GPS application," *Journal of Electromagnetic Waves and Applications*, Vol. 24, Nos. 8–9, 1033–1044, 2010.
23. Li, W. M., Y. C. Jiao, L. Zhou, and T. Ni, "Compact dual-band circularly polarized monopole antenna," *Journal of Electromagnetic Waves and Applications*, Vol. 25, Nos. 14–15, 2130–2137, 2011.
24. Im, Y. T., J. H. Kim, and W. S. Park, "Matching techniques for miniaturized UHF RFID loop antennas," *IEEE Antennas Wireless Propag. Lett.*, Vol. 8, 266–270, May 2009.
25. Kang, J. J., D. J. Lee, C. C. Chen, J. F. Whitaker, and E. J. Rothwell, "Compact mobile RFID antenna design and analysis using photonic-assisted vector near-field characterization," *Proc. IEEE Int. Conf. RFID*, 81–88, Apr. 2008.